Modelling Thermal Performance of Unloaded Spiral Strand and Locked Coil Cables Subject to Pool Fires

As published in Structural Engineering International

2022

Doi: 10.1080/10168664.2022.2101969

(Manuscript Author order: Watson, Nicoletta, Kotsovinos, Al Hamd, Gales)

John Gales PhD (Principal Investigator, York University)
Scott Watson (Research Student, University of Waterloo)
Ben Nicoletta (Research Student, York University)
Panagiotis Kotsovinos (Arup)
Rwayda Al Hamd (Abertay University)

Abstract

Structural cables are often used to design critical structures such as bridges. Cable supported bridges are not typically redundant; a loss or compromise of a few cables can lead to the progressive collapse of an entire cable-supported bridge, causing economic harm, loss of property and, in extreme cases, loss of life. Additionally, previous experimental research has shown that the degradation of material properties and thermal expansion of structural cables is more onerous than the standard carbon prestressing steel. Despite its importance for the design of cable-supported structures, no well-validated methodology exists to aid in the thermal performance of structural cables in the event of a fire, particularly for spiral and locked-coil cables which inherently are complex due to their cross-sectional geometry. The novelty of this project is that addresses this knowledge gap by developing a state-of-the-art methodology for modelling structural cables' thermal response which addresses the difficult to model nature of bridge spiral and locked-coil cables. The usefulness of the methodology is that it will enable the development of an understanding of the temperature distribution and thermal deformation in a cable cross-section, and it will further allow subsequent estimation of post-fire resilience in a fire event. The methodology developed herein benefits with its validation for the first time against previous experiments of locked-coil and spiral strand cables, subjected to realistic pool fires. The cables range from 22 mm to 100 mm in diameter and are constructed out of galvanized or stainless steel. The cables are modelled undergoing a non-linear thermal analysis in LS-DYNA. By comparing the numerical results of 2D and 3D models to experimental results, the method's validity is verified in its ability to predict maximum temperatures and general trends of heat exchange between the strands. 2D models are found to provide conservative estimates for critical values such as peak temperature with 90% accuracy, while 3D models provide slightly more conservative estimates. The paper concludes with a research needs framework for understanding the thermal-structural deformation response of spiral and locked-coil cables bridge types.

Keywords: Structural Cables, Bridges, Thermal Analysis, Finite Element Analysis, Nonlinear

Table of Contents

1. Introduction

Structural cables (see Figure 1), including parallel strand, locked-coil, and spiral strand varieties, are prevalent in structures, such as bridges, airports, stadia, and train station platforms [1]. Although bridges and other cable-supported structures often comprise critical infrastructure, the methods for determining the fire resistance of these structures are not well developed, partially due to a lack of incentive to enhance the fire resilience for low-probability events that have not been traditionally considered in design. Bridge design against fire events is rarely considered despite the probability for fires affecting bridge structures to be high enough to be considered a potential risk, per Naser and Kodur [2]. A state-of-the-art literature review conducted by Garlock et al. [3] reinforces the lack of fire-safe bridge design, citing the lack of guidance in American and European standards. Additionally, the concern is raised on the effects of hydrocarbon fires, such as petrol fires, which can reach high temperatures within a few minutes of ignition [3]. Quiel et al. [4] built off the concerns of Garlock et al., citing gasoline and diesel tanker trucks as being responsible for recent fire events involving bridge structures, namely the MacArthur Maze interchange overpass, the I-65 overpass near Birmingham, and the near-collapse of the Route 22 overpass at I-81 near Harrisburg. Quiel et al. [4] developed a method for determining the fire response of steel elements supporting a fire-exposed bridge using results from the MacArthur Maze overpass to validate the results. In addition, the effect of a truck fire on the main cable of the New Little Belt Bridge in Denmark had been analyzed, highlighting that these fires can lead to a reduction in cable strength or failure, threatening the integrity of the bridge [5]. With this, a systematic approach to fire protection of main cables has been outlined and implemented for large suspension bridges [5]. As a whole, the knowledge of the response of bridge structures to fire has only been targeted within the past 15 years and, while progress has been made, knowledge gaps persist that limit practitioners' abilities to design fire-resilient bridges. This is especially true for the case of cable-supported bridges and cable-supported structures in general. Cables used in these structures are complex elements and there is a lack of understanding concerning the thermal response, in terms both of material properties and structural behaviour, of structural cables exposed to fire [6]. This is cause for concern as the loss of a few cables can lead to total failure and collapse of the structure, which can have an adverse economic impact and potential loss of life [7]. Previous research has shown the weaknesses of these cables when exposed to fire, indicating that necessary design methodologies and guidance in a fire-safe objective and performance-based environments are needed [8-11]. There is a dearth of research available on the fire response of cable-stayed structures.

Figure 1. Stay cable as installed in a bridge in Calgary, Canada and in a building under construction in Winnipeg, Canada (Authors Photos)

Efforts have begun to study the effects of structural cable loss for cable-stayed bridges [12]. In these studies, it is shown that the loss of a few cables can lead to the progressive collapse of the entire structure. However, those studies did not assess the cable performance directly. Additionally, previous experimental research illustrated the degradation of material properties being more pronounced than current models predict [13], highlighting the danger of underlying damages that may remain apparent after a fire has been extinguished. To predict the heat transfer and potential damage to the structural cable, finite element modelling (FEM) can be used to analyze the heat transfer within a provisional first step in more holistic design methodology development. FEM can offer a faster, less resource-intensive method for acquiring engineering approximations for the problem at hand, providing it is validated and verified to give acceptable predictions. When applied to structural cables exposed to fire, temperatures perceived across the model are visualized, allowing for informed, risk-based decisions to be made during the design process.

Naser and Kodur [2] suggest using an 'importance factor' when designing bridges for fire resistance. The 'importance factor' is most dependent on the geometric feature of the structural component, among other factors such as potential threats and economic impact [2]. Milne determines the arrangement of wires and wire geometry to influence the heat transfer and get reliable thermal predictions [14]. The importance of geometric features in fire design has led to the experimental methodologies conducted by Nicoletta et al. [15] providing reliable and realistic in-scale data concerning the relation between cable geometry and its thermal response. Though important, an experimental research programme is costly, requiring time and resources from stakeholders. Therefore, developing a novel modelling approach that can capture the behavior of the structural cables under fire is crucial. Despite the availability of other numerical methods, the finite element method holds an advantage in design practice through its ability to provide solutions to irregular geometries with unusual boundary conditions. In addition, once a reliable model has been developed, the effect of minor changes can be studied, such as changes in geometry or material [16]. Knowledge on the effect of these changes can lead to a faster and less expensive design process, producing higher quality products with a lower chance of failure when

in use, as determined by Rao et al. in a literature review on the applications of the finite element method [17].

A numerical model is required to assess the thermal response of unloaded structural cables, i.e., the cross-sectional temperature distribution capturing the heat transfer through the air gaps, which adds more complexity to the model. The development of a model provides a platform to study the effects changes in variables have on the results, allowing for more informed design choices. FEM also offers practitioners a way to break down complicated behaviours to identify the more specific parameters and scenarios that can govern the design and later tailor a resulting hand calculated solution for day-to-day use. Heat distribution can provide valuable insight into potential effects on mechanical properties, such as thermal expansion, thermal bowing, creep, and residual stress relief, which can have unexpected consequences on affected cable-stayed structures [15]. According to Du et al. [1], with the end goal of developing a valid methodology for the structural-thermal analysis of loaded cables, a valid heat transfer model is essential, constituting the preliminary step after designing the cable and the localized fire condition, following their methodology for designing pre-tensioned cables exposed to a localized fire [1]. The thermal response of loaded cables requires additional research and thus lacks the data necessary to verify and validate a potential finite element model.

This paper proposes a state of the art methodology for the analysis of the thermal response of unloaded spiral strand and locked-coil structural cables exposed to realistic localized fires and validates it based on previous experimental results. To verify and validate the proposed methodology, locked-coil and spiral strand cables, ranging from 22 mm to 100 mm in diameter and constructed out of galvanized steel or stainless steel, are modelled and undergo a non-linear thermal analysis using LS-DYNA. A non-linear analysis is performed to account for the temperature-dependent material properties and the non-linear nature of radiation boundary conditions. The results obtained from LS-DYNA are verified and validated against experimental data obtained by Nicoletta et al. [15], who studied the thermal response of structural cables exposed to a methanol pool fire. To the best of the authors' knowledge, no prior validation of a model exists in the literature for large diameter spiral and locked-coil strands subjected to realistic localized pool fires. The model herein uses LS-DYNA, selected for its extensive use in both academic and industrial fire sectors [18] . Despite the use of LS-DYNA, the proposed model is applicable to all FEM software that can capture the relevant physics subject to appropriate validation.

This research forms part of a greater framework to advance the knowledge of the fire response of structural cables and ultimately contribute to the design of fire-resilient cable-supported infrastructure. In a state-of-the-art review of the thermal performance of structural cables, Kotsovinos et al. indicate that, of the limited experimental studies performed, regarding the fire performance of cable members, only that by Nicoletta et al. considered non-uniform heating of cable diameters greater than those used in prestressed concrete construction and at a heating rate suitable for the development of large thermal gradients [6,15]. Cables under this heating configuration represent a realistic and critical case where non-uniform temperature gradients (both cross-sectionally and longitudinally) occur which can complicate the thermomechanical response by creating thermally-induce moments and potentially causing localized uncoiling and complex load-shedding. Therefore, the novelty in the experimental study

by Nicoletta et al. is shared by the modelling efforts herein which attempt to generalize the experimental results and provide a tool for determining the thermal response of structural cables under this critical non-uniform condition and to further investigate these important and complex second-order effects. Moreover, the modelling efforts herein attempt to fill the critical knowledge gaps identified by Kotsovinos et al., including furthering the understanding of the development of thermal strains in the cable structure, the response of structural cables to non-uniform fire exposures, and more broadly to the fundamental thermomechanical performance of large-diameter cables. This work contributes to the greater research framework undertaken by the authors which serves to characterize the thermal and mechanical performance of cable elements and culminates in combined thermomechanical testing and modelling. This framework will yield more efficient performance-based design tools for the fire design of cable-supported structures.

1.1 Experimental Data Sets

The results of the finite element models are verified and validated against the authors' previously acquired experimental data [15]. This data is chosen as it covers a broader range of cable diameters used in construction and is readily available to practitioners in detail [19]. Through the literature review conducted by Kotsovinos et al. [6] and Nicoletta et al. [15], knowledge gaps exist concerning the thermal response of cables with diameters larger than 80 millimeters. Using cables provided by global manufacturers, cables ranging from 22 mm to 100 mm in diameter are exposed to a methanol pool fire, confirming previously available test data while filling in existing knowledge gaps. Temperature readings are taken at various locations along the cable to map the temperature profile and deformations caused by thermally induced stresses on the cables.

This experiment does not measure the mechanical effects of the heat source, and the cables studied are unloaded. The experiment results serve as a foundation for an eventual structural-thermal model, whose need is demonstrated elsewhere by Kotsovinos, Judge, et al. [6].

These original experiments placed thermocouples on cable top and soffit surfaces, and in cable core wire. Therefore, the original experiments do not provide as many temperature readings as a typical model would. Since top and soffit surface measurements are used as temperature boundary conditions, the only data left to validate the model herein will be the core wire temperature readings. The thermal gradient is important from a structural perspective. It will be expected that for the core temperature to be accurately modelled, an accurate gradient would need to be modelled, since heat transfer rate through the cable is dictated by the temperature difference between the cable surface and core wire.

1.2 Existing Cable Modelling

As of the writing, limited guidance exists on the computational thermal analysis of structural cables. Current literature focuses on the structural design of cables at ambient conditions, ranging from studying bridge response following stay cable breakage to the structural finite element analysis of the stay cables. Despite this, these analyses are relatively scarce. A method for validating the thermal response of parallel strand structural cables exposed to fire is suggested by Kotsovinos et al. and Lugarsi [20,21]. The method proposed by Kotsovinos et al. is relevant to parallel strand cables and is different from the method employed in this paper,

notably considering different geometry with different heat transfer characteristics. Kotsovinos et al. propose a methodology for analyzing parallel strand cables, whereas the methodology presented herein focuses on locked-coil and spiral strand cables. Though a different method is suggested, Kotsovinos et al.'s approach has been used as a basis in the attempt to develop the proposed model. A method for the numerical analysis of locked-coil cables exposed to fire has also been developed [22] using experimental structural and thermal loads; thus developing a thermal-structural model emphasizing the effects of temperature on stress-strain relations. In contrast, the methodology presented in this paper focuses on the thermal response of unloaded cables. Additionally, the proposed model is validated against experiments of large diameter cables subject to pool fires in this work. The importance of 2D and 3D representation is also investigated.

Quiel et al. [23] proposed a simplified model that does not capture the thermal gradient in a cable as it focuses on the effects of fire protection on mitigating the heat transfer in bridge cables due to fire caused by a tanker truck fire. Other notable modelling efforts for structural cables focus on estimating their structural behavior. Fontanari et al. [24] developed a model for the Warrington-Seale rope. Structural cable modelling has also been performed on pre-tensioned steel cables exposed to fire [1], emphasizing the structural response such as the effects on Young's Modulus and the stress-strain relationship. The results and procedures followed to develop these models would make the first steps in developing a structural-thermal model for spiral-strand and locked- coil cables.

2. Methodology

2.1 Geometry

The experimental evidence by Nicoletta et al. [15] is based on the nine samples provided by three global manufacturers. Of the nine samples, six are selected to develop the numerical models (Table 1). The cables follow a spiral or locked-coil design, are made of galvanized or stainless steel and range from 22 to 100 millimetres in diameter (Figure 2). Each layer constitutes several strands, shown under 'Strand Labelling' (Table 1). Strand layers depicted with a 'Z' represent layers linked through z-links, named after their unique shape. The z-layers are assumed to display perfect contact in the models and are thus modelled as a solid, hollow cylinder during geometry creation. The naming of the specimens follows a format. The first letter describes the cable type, spiral (S) or full locked-coil (L). The following two letters depict the material used, galvanized steel (GS) or stainless steel (SS), and the final set of numbers is the nominal diameter of the specimen. Two specimens are provided for the 100 mm diameter cables. They are differentiated by an 'A' or 'B' following the diameter. Note the unique strand labelling of both L-GS-100 specimens. The bolded numbers separated by a forward-slash represent the two different strand sizes within the same layer (i.e. 6 larger wires with 6 smaller wires in the gaps between for sample L-GS-100 A/B).

Table 1. Cable cross-sections dimensions

Specimen Name	Nominal diameter (mm)	Cable Type	Strand Labelling	Strand Dimensions (mm) Diameter (D) for round strands Height (H) of Z-strands
S-SS-22	22	Spiral	1 + 6 + 12 + 16	Round (layers 1-4): D = 3 mm
S-SS-50	50	Spiral	1 + 6 + 12 + 18 + 25 + 32 + 42	Round (layers 1-7): D = 4.25 mm
L-GS-70	70	Locked-Coil	1 + 6 + 12 + 18 + 24 + (30 + 36 + 42) Z	Round (layers 1-5): D = 4.5 mm Z (layers 6-8): H = 5 mm
S-GS-74	74	Spiral	1 + 6 + 12 + 18 + 24 + 30 + 36 + 33 + 39 + 45	Round (layers 1-7): D = 3.75 mm Round (layers 8-10): D = 4.6 mm
L-GS-100-A/B	100	Locked-Coil	1 + 6/6 + 12 + 18 + 24 + 30 + (44 + 44 + 50 + 56) Z	Round (layers 1-6): D = 4.5 mm Round (layer 2 smaller): D = 2 mm Z (layer 7): h = 4 mm Z (layers 8-10): h = 5 mm

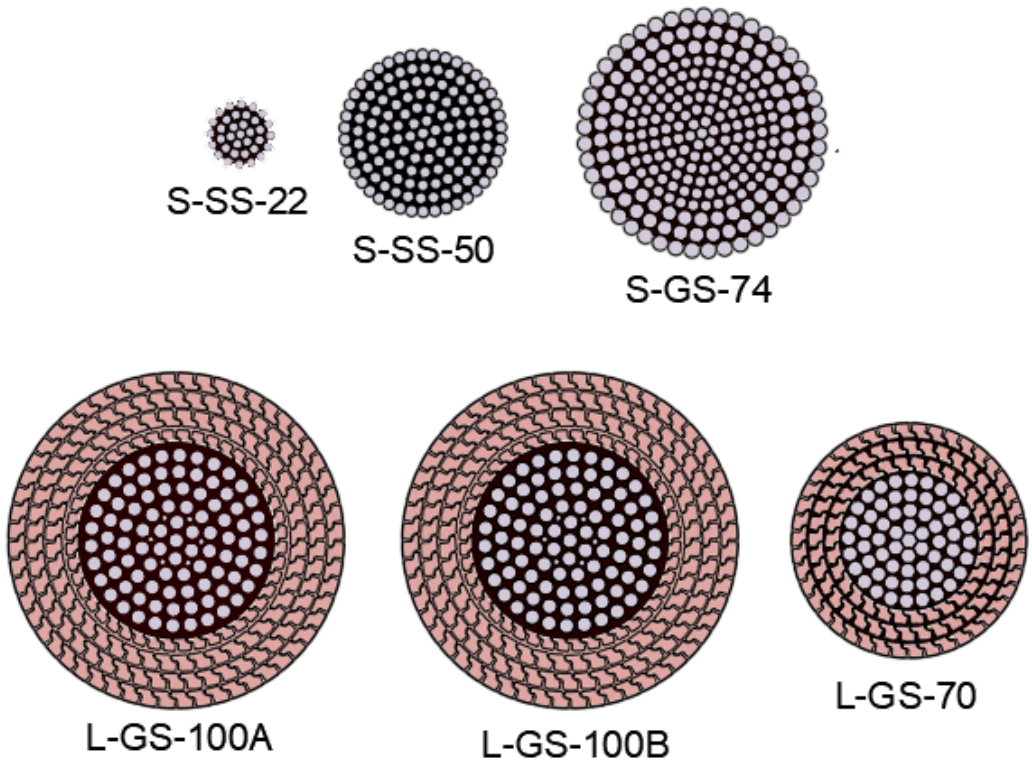

Figure 2. Cross-section drawings of cable samples (adapted from [15])

Figure 3. Cross-section view of L-GS-100A (left) and L-GS-100B (right) experimental sample, taken after experimental testing

Visual analysis (Figure 3) of the physical samples shows the individual strands are much more closely packed than the manufacturer's specifications. Thus, to accurately capture the as-built cable geometry, manufacturer's specifications are referred to for wire diameter only, and layers are packed as closely as possible. Note that the cross-section of L-GS-100A and L-GS-100B (Figure 3) were similar before being tested. The denser cross-sections of the as-built cables are attributed to the need to tightly wind the ends of the cable to prevent unravelling of the strands.

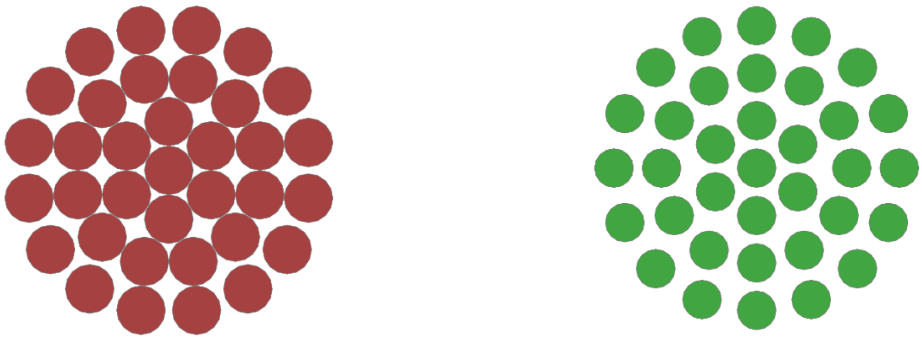

Figure 4. Tightly packed (left) vs manufacturer-specifications (right) models

As will be discussed, a method to model heat transfer between the wire strands is conductivity through the fluid between the wires. A preliminary test of the effect wire proximity has on the results, analyzed using tightly-packed and manufacturer-specification models (Figure 4), shows significantly more satisfactory results for the model with tightly packed wires (Figure 5). The improved results are also tied to the use of Contact cards to represent heat transfer between the gaps, which are highly dependent on model geometry. Contact card setup is covered in detail in a subsequent section. A geometry following the manufacturer's specifications heats and cools slower than the experimental results, whereas a tightly packed geometry accurately

represents the heating and cooling of the model and provides conservative estimates around higher temperatures.

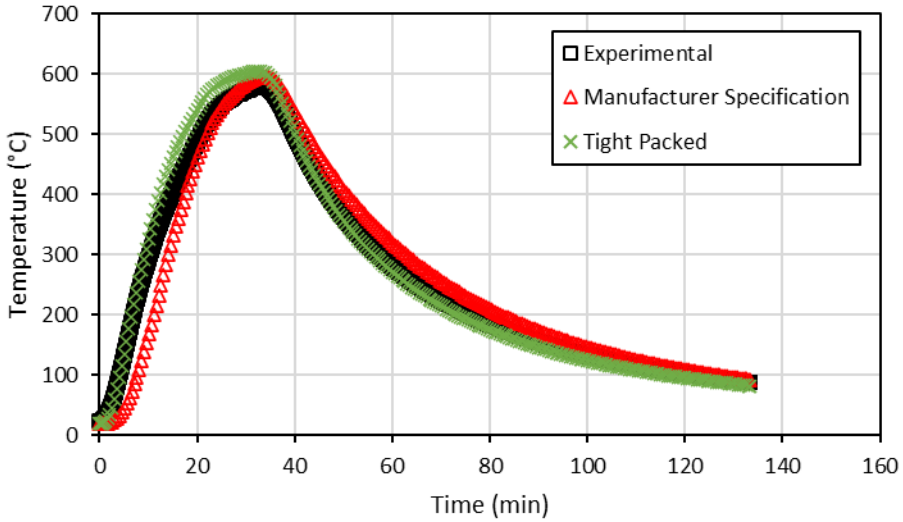

Figure 5. Effect of geometry on core temperature results for S-SS-50

Following these results, all other models are created such that the wires are as tightly packed as possible. The 'tightly-packed' configuration is achieved by reducing layer diameters until either wire contact those in the inner layer, or if wires contact adjacent wires in the same layer. Manufacturers' specifications are used as guides, primarily for the diameter and thickness of each layer. It should be noted that modelling in a close-packed configuration yields smaller cable diameters than those provided by the manufacturers. In addition, visual inspection of the samples shows that particular layers have less strands per layer when compared to the manufacturer's specifications (Table 1). Therefore, the number of strands per layer has been adjusted accordingly, removing only one or two strands in a layer at most in order to get the desired tightly packed geometry.

2.2 Cable Specimen Model Creation

The proposed methodology is intended to be applicable to the software package of the practitioner's choice. SolidWorks was used for geometry generation, HyperMesh was used to generate the mesh, and a Primer tool was used for material property and initial and boundary condition application. A graphical representation of the procedure followed, and software used is included (Figure 6) and detailed below.

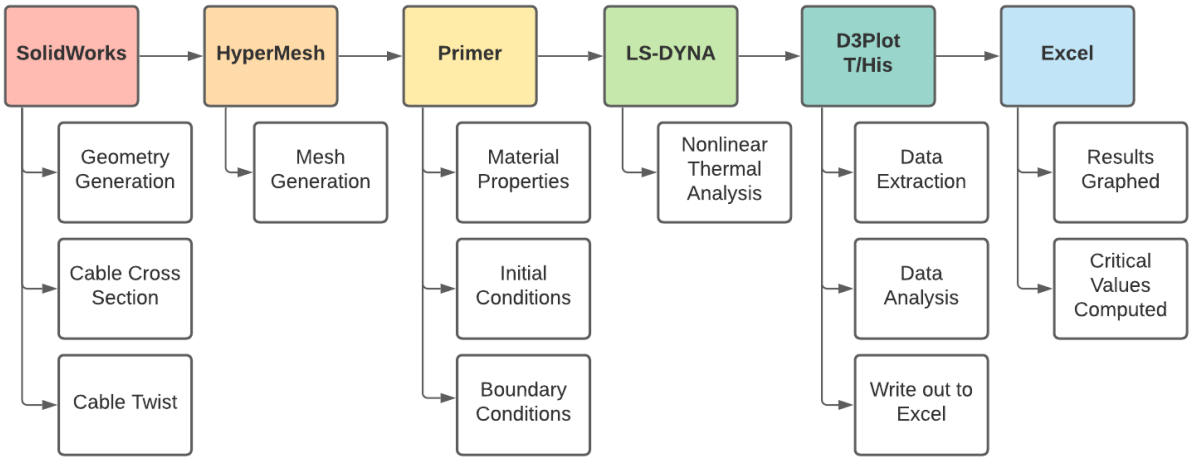

Figure 6. Graphic of software used and their respective contribution to the thermal analysis process

2.2.1 Model Geometry

The full 3D geometry is created in SolidWorks. An accurate cross-section geometry is created using data on the cable geometries (Table 1). The strands are then extruded using a Sweep function, with the outer strands twisting around the central one in a sweeping motion. The direction of the twist is assumed to alternate between layers (see Figure 7).

An analytical approach is used to identify the pitch angle. By taking manual measurements of experimental results [15], the angle of the strand relative to the horizontal is identified and used as the pitch angle. Since the cable elongates as the experiment progresses, [15] only the first few frames are used to get an accurate length measurement. The pitch angle is verified to be the same for all underlying cable-layers. An example length measurement is shown (see Figure 8). The length measurements and calculated pitch angles for each specimen are tabulated (see Table 2). Refer also to Supplemental Material A – Pitch Angle Measurements for measurements taken for each sample.

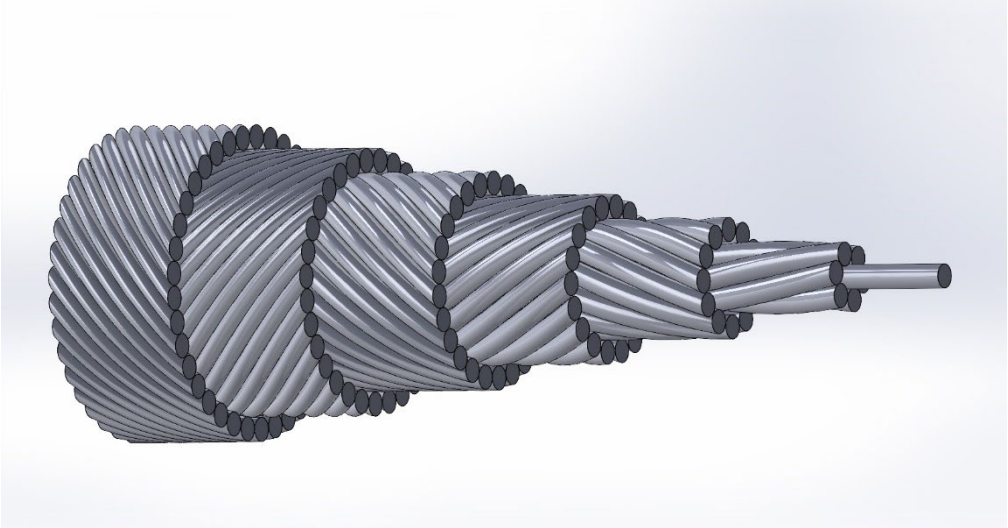

Figure 7. Exposed strands of CAD model for S-SS-50. Exaggerated pitch angles are used to visualize the alternating twist direction of each layer and differ from those used in the analysis (as adapted from [25])

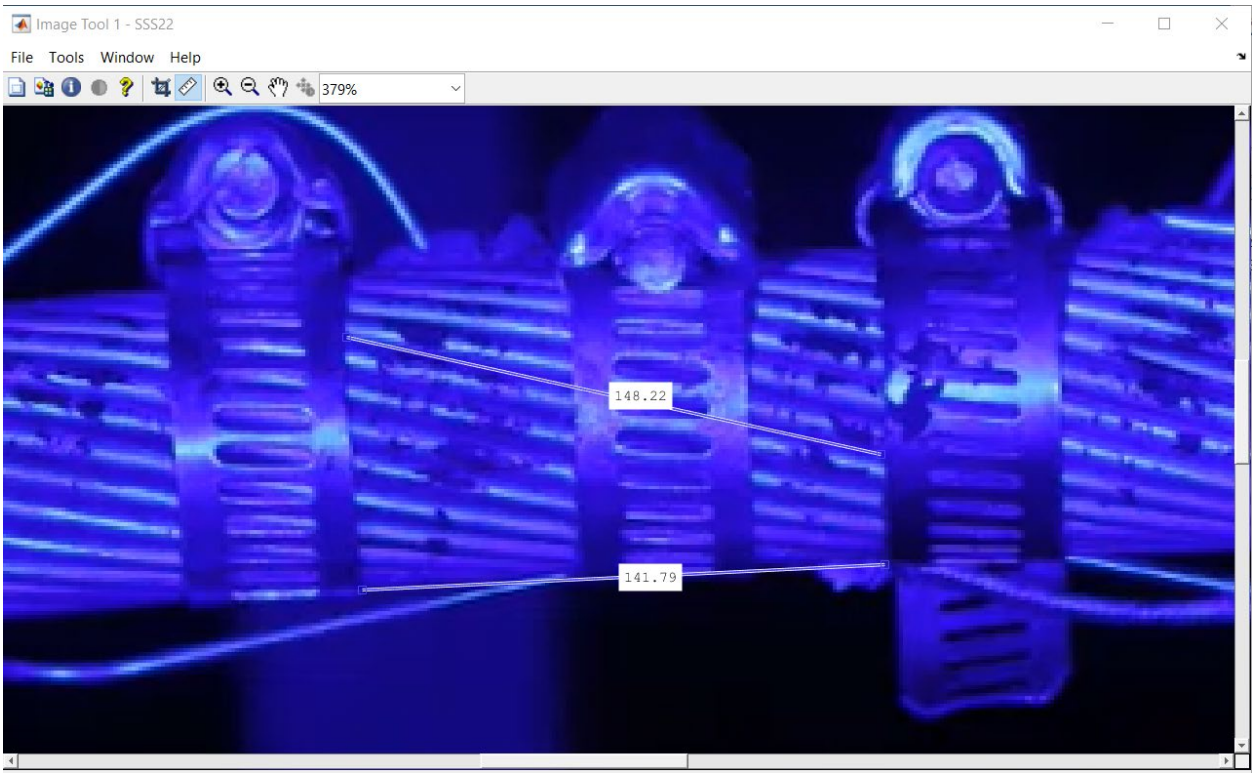

Figure 8. Horizontal and diagonal pixel length measurements are taken in Matlab for sample S-SS-22. Values are then used for the calculation of the pitch angle.

Table 2. Horizontal and diagonal length measurements taken in Matlab and the calculated pitch angle for each sample

Sample Number	Horizontal Measurement (mm) (Adjacent)	Diagonal Measurement (mm) (Hypothenuse)	Pitch Angle (°) $\theta = \cos^{-1}\left(\frac{Adjacent}{Hypothenuse}\right)$	Coating
S-SS-22	141.79	148.22	16.94	Stainless Steel
S-SS-50	163.22	181.20	25.74	
S-GS-74	158.04	167.66	19.49	Galvanized Steel
L-GS-70	170.59	184.52	22.41	
L-GS-100-A	168.77	188.58	26.50	
L-GS-100-B	326.64	362.59	25.73	

2.2.2 Model Mesh

The geometry created from SolidWorks is imported into HyperMesh, and two types of meshes are created; a mesh of the cross-section, used for the 2D analysis, and a mesh of the entire geometry, used for the 3D analysis. The creation of the 2D mesh is simple. The desired mesh size is inputted, and HyperMesh populates the surfaces with the specified mesh parameters. The mesh sizes used and how they are determined are discussed in further detail in the following section.

A 'solid map' tool in HyperMesh was used for meshing 3D geometries. This allowed meshes to be extrapolated over a defined path. Initial efforts focused on meshing each layer individually to account for the alternating twist directions of each layer. The meshing of each strand was performed individually to avoid errors in volume.

Mesh Size

The authors approached the sensitivity analysis by analyzing the results of 2D and 3D models for the smallest and largest diameter models at varying mesh sizes for the cross-section and along the length of the 3D model. In doing so, a maximum and minimum mesh size is determined, and all other sizes are expected to fall within the defined range of values.

To determine an appropriate mesh size for the models, a mesh sensitivity study is conducted, weighing peak temperature error and CPU time as relevant factors against a range of mesh sizes. Following the results of the sensitivity analysis, the cross-sectional mesh is found to have negligible effect on the peak temperature accuracy. Hence, more emphasis is made to choose a mesh size fine enough to accurately describe the geometry. Thus, S-SS-22 and L-GS-100 are given a cross-section mesh size of 0.6 and 0.9mm, respectively.

A similar analysis is conducted to determine an appropriate element longitudinal size for the 3D models. The results of the analysis suggest that an element longitudinal size of 50mm is appropriate for S-SS-22 and L-GS-100 3D analyses. Detailed mesh sensitivity analyses for 2D mesh size and 3D element size are included in Supplemental Material B – Mesh Sensitivity Study.

However, the proposed sensitivity study leaves room for improvement. Experimental uncertainties have yet to be quantified, making the comparison of experimental and numerical results a challenge. Future work may consider the determination of such experimental uncertainties to refine the mesh sensitivity analysis. Furthermore, study is required to determine model stability by verifying the model's ability to converge to specified values by modifying mesh size.

Mesh Transition

A coarse mesh is used at the surface for the locked-coil models, whereas the finer mesh size determined through the sensitivity analysis is used towards the center. The use of a coarse mesh simplifies the analysis and greatly reduces CPU time. To use two different mesh sizes within a single model, a smooth transition must be created between the two sizes so that all nodes connect [26]. Once a mesh size is inputted, HyperMesh automatically assigns a recommended mesh that best represents the input parameters. Along the contours of the recommended mesh, the number of nodes are shown and can be altered. To create a transitioning mesh, a 2:1 ratio is defined between the locked-coil layers' outer and inner surface nodes. The selected ratio generates one of multiple mesh transition techniques (see [26]), decreasing computational time without sacrificing results accuracy. The 2:1 ratio is achieved by halving the number of nodes on the outer surface. HyperMesh then updates the recommendation based on the new parameters, and the new recommended mesh is used. This method is not applicable to the spiral strand cables as uniform mesh size is used across the entire model.

2.2.3 Material Properties

Oasys Primer is used to specify material properties, initial and boundary conditions and details on the analysis, such as analysis time and time step size. 2D and 3D models are set up. The density, thermal conductivity and specific heat of the material are defined for the model. The density is assumed to be independent of heat, whereas thermal conductivity and specific heat are treated as temperature-dependent. Data on material properties are taken from EN 1993-1-2 [27]. EN 1993-1-2 does not provide material properties for galvanized steel. Instead, carbon steel is assumed to provide adequate representation for the behavior of galvanized steel, since galvanized steel is carbon steel coated in a layer of zinc. The process of hot-dip galvanizing creates a zinc layer on the surface, providing corrosion protection to the steel substrate [28]. Rao et al. study the effects surface coatings have on the thermal performance of steel substrates, concluding that the coatings provide marginal heat resistance, altering the heating rate by only a few degrees [29]. Therefore, the zinc coating is ignored in the development of the models as the underlying steel is not affected by the zinc surface coating.

Initial Conditions

The initial condition defines the temperature of the model when the analysis begins. In general applications, it is assumed that the model is stored at room temperature for a substantial amount of time, allowing the model to reach equilibrium at room temperature. Each sample is assumed to be at room temperature ($20℃$) before the experiment is conducted. Experimental results show the initial temperature varies for each sample though the room temperature initial condition is shown to be a valid assumption.

Geometry Modification

Next, the model is cut in half along its length to decrease the model size and subsequently decrease the required CPU time. During the experimental analysis, the full specimen length is propped over a pool fire, exposing a 500 mm wide area in the center and insulating the ends of the cable [15] . Such a setup creates a line of symmetry along the cable's centre as heat transfer is expected to be similar on both sides. Therefore, splitting the geometry along the axis of symmetry yields accurate results.

Solver and Time Step Size

All models undergo a thermal-only, fully implicit analysis in LS-DYNA and are analyzed using a diagonal scaled conjugate gradient iterative solver [30-32].

A variable time step is used and is determined based on the change in temperature, which occurs within a timestep. The timestep is initially set to 1.0 sec. If the temperature change is larger than 50 Kelvin, the timestep is re-analyzed using a smaller timestep. LS-DYNA continues to decrease the timestep size until either the temperature change criteria is met, or a user-defined minimum timestep size of 1.0E-6 second is met, at which point the analysis terminates. If the temperature change is less than 50 Kelvin, the timestep increases up to 50.0 second while ensuring the maximum temperature change criteria are still met [15] . Using a variable timestep ensures the optimal timestep is always being used, minimizing analysis time while ensuring a smooth temperature change every time.

When solving non-linear problems, LS-DYNA uses Newton's method to determine the solution curve. The Newton method often diverges, leading to a pre-emptive termination of the analysis without any meaningful results being outputted. LS-DYNA reduces the time step by a fraction of a solution diverges, determined using a "line search" optimization method.

Heat Transfer Between Strands

Primer is used to define the driving forces of the analysis. LS-DYNA uses a 'Contact card'. A Contact card measures the gap between surfaces and splits the gap into three regions, based on user input. The first region assumes the two surfaces are in contact and conductance is the primary form of heat transfer. The second region assumes a gap exists between the surfaces but are still close enough for heat transfer to occur via conduction through air between the gaps and radiation across the gap. The final region assumes the two surfaces are too far apart for any heat transfer to occur, and thus the two surfaces do not interact (Figure 9).

$$\begin{cases} \text{Closed gap conductance} & 0 \le l_{gap} \le l_{min} \\ \text{Conductance through fluid + radiation} & l_{min} < l_{gap} \le l_{max} \\ \text{No heat transfer} & l_{gap} > l_{max} \end{cases}$$

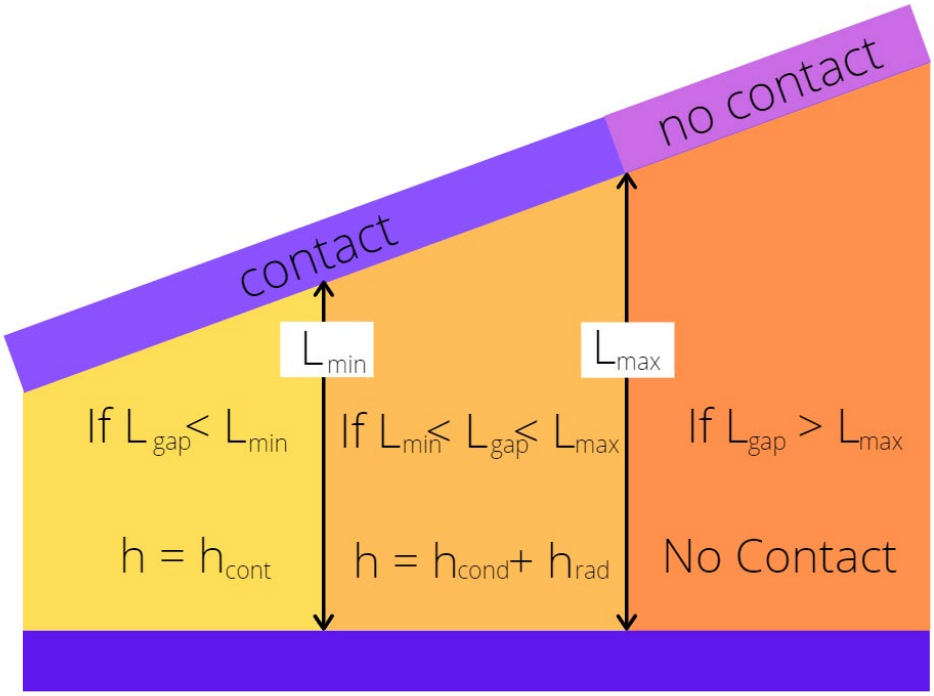

Figure 9. Visual representation of the LS-DYNA Contact card, adapted from Shapiro [28]

Initial analyses yield aggressive heating and cooling and higher peak temperatures compared to the experimental results. This was initially thought to be caused by the conductance between strands in the $0 \leq l_{gap} \leq l_{min}$ region as the air between the gaps was expected to act as an insulator compared to the direct heat transfer between wires.

A sensitivity analysis is conducted to test this theory (see Supplemental Material C – Closed Gap Conductance Sensitivity Analysis). By setting l_{min} to zero, the requirements for the first region are never met, ensuring only conduction through the fluid and radiation are the driving factors for heat transfer. The sensitivity analysis results show no correlation between the final results and the conductivity through contacting strands, suggesting conductivity through the air cavities and radiation through the gaps to be the driving mechanisms for heat transfer. All subsequent models omit the conductance through contacting strands.

To reduce the increased heating and cooling rates, only two inputs can be altered by the user: the radiation factor or the thermal conductivity of the fluid. The radiation factor is determined using the following equation:

$$f_{rad} = \frac{\sigma}{\frac{1}{\varepsilon_1} + \frac{1}{\varepsilon_2} - 1}$$

Where σ is the Stefan-Boltzmann constant ($5.67E-8\ [W/m^2K^4]$) and $\varepsilon_{1,2}$ are the emissivity of the 'master' and 'slave' surfaces, respectively. Since all values are either constant or material dependent, the radiation factor can not be changed to lower the heat transfer between wires.

The remaining parameter to be altered is the thermal conductivity of the air between the surfaces. Initial analyses are performed using the thermal conductivity of air at high

temperatures, around the maximum temperatures experienced by the samples. Another set of analyses is performed using the thermal conductivity of air taken at room temperature, this time yielding insufficient heating and cooling, sometimes yielding lower peak temperatures (see Supplemental Material D – Fluid Thermal Conductivity Sensitivity Analysis).

Due to the high dependency of the results on the thermal conductivity of the air in the cavities, a new value is taken at the average temperature experienced throughout the analyses. Ideally, a thermally dependent value is defined, though LS-DYNA does not provide this functionality when using Contact cards. The results obtained using the thermal conductivity of air at the average expected temperature is significantly more favorable, as shown against other thermal conductivity values (see Supplemental Material D – Fluid Thermal Conductivity Sensitivity Analysis).

It is noted that the dependence mentioned above on the thermal conductivity of air is most prominent in large diameter cables. Smaller diameter cables such as S-SS-22 show no change in result when using thermal conductivity values at different temperatures.

All models are analyzed with $l_{min} = 0$ and $l_{max} = 0.004\ m$. As previously mentioned, l_{min} is selected to ensure conduction through the fluid and radiation are the driving mechanisms of heat transfer. The upper bound, l_{min}, is determined via measurement of physical samples and CAD models, such that heat transfer only occurs between strands directly across one another in neighbouring layers.

Boundary Conditions

A temperature boundary condition is applied for initial analyses corresponding to the experimental top and soffit temperatures, with the upper half surface being the top and the lower half surface being the soffit. Constant top and soffit temperature boundaries are applied to the nodes located on the outermost circumference of the model, thus yielding a temperature gradient through the center (see Figure 10). Such a method is used to verify and validate the heat transfer between strands. Despite the assumption of uniform temperature on the top and soffit surfaces and the sudden temperature change at the intersection of the two boundaries, the model displays favorable heat transfer between the strands and core temperature results match those determined experimentally.

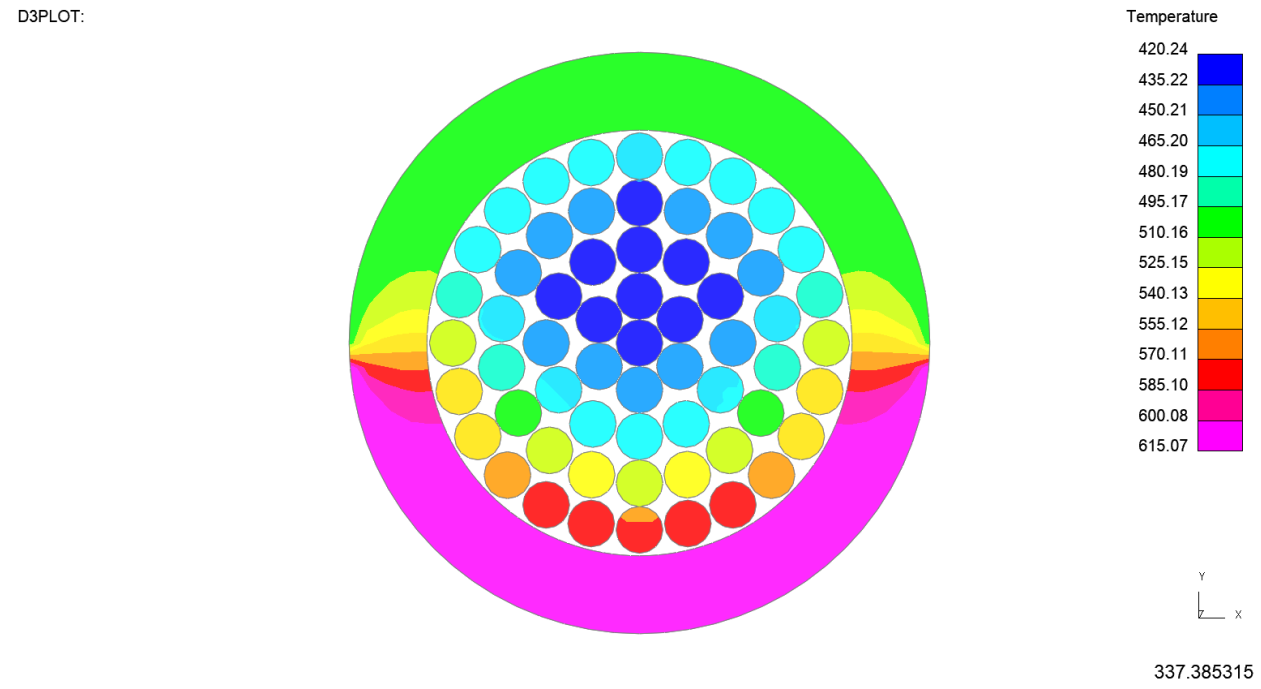

Figure 10. L-GS-70 2D model split into top and soffit boundary conditions, taken 5,6 mins into analysis

3. Results

3.1 Two-Dimensional Models

Nicoletta et al. [15] use samples S-GS-44 and S-GS-82 as preliminary tests to identify potential challenges with instrumentation and the experimental methodology. The top thermocouple measures the gas temperature instead of measuring the top surface temperature recorded for all other samples. Since the results in this section rely on experimental top and soffit temperatures to test the validity of the heat transfer model between strands, the use of gas temperature is unjustifiable and yields significantly higher core temperatures. As such, the results of S-GS-44 and S-GS-82 are omitted from this section. In addition, the results of L-GS-140 are not included due to uncertainty in thermocouple placement near the core of the strand for experimental sample L-GS-140. Results of the 2D LS-DYNA models are shown in Figure 11.

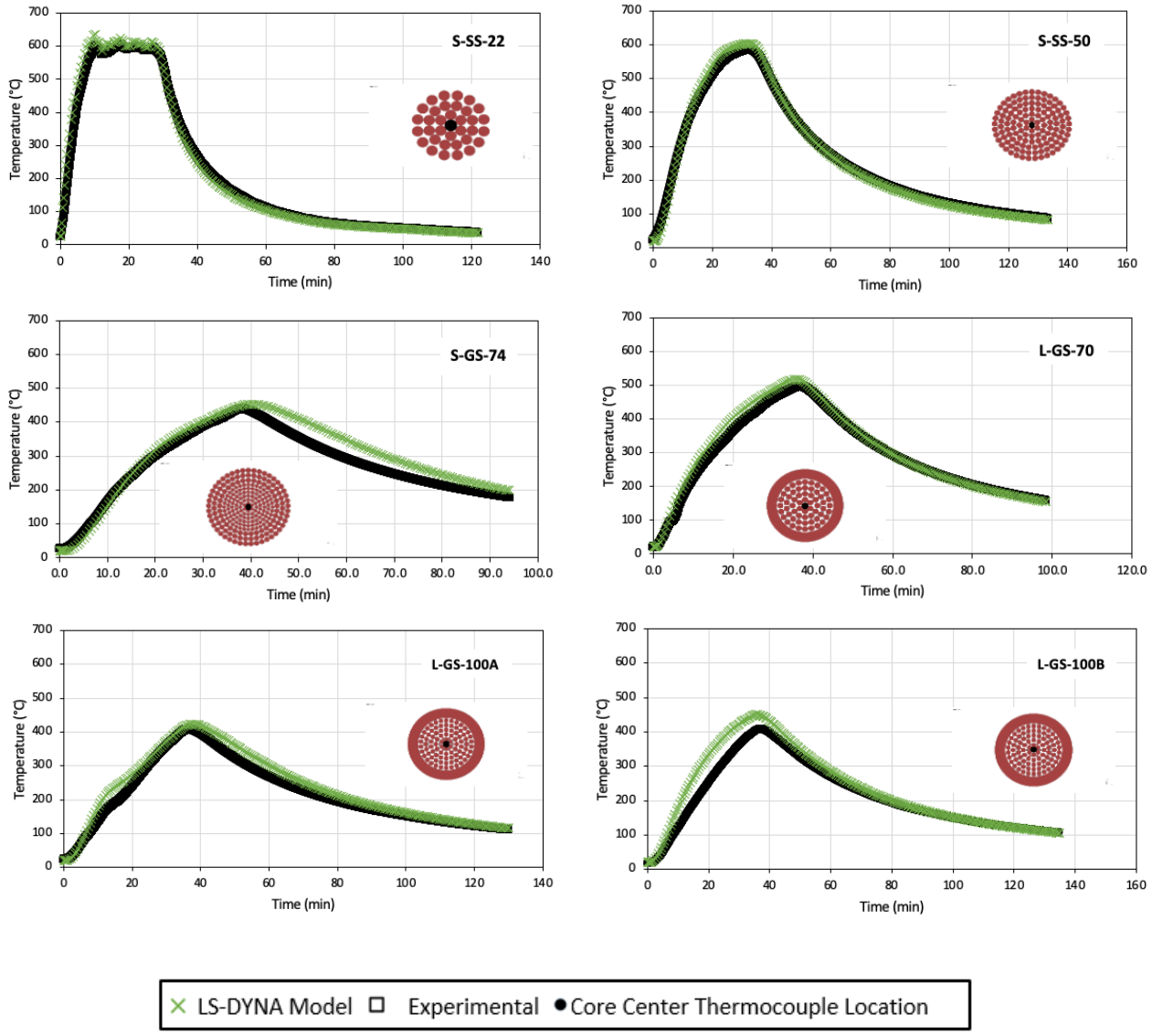

Figure 11. 2D Core Centers Calculated and Experimental Temperatures

Model results are compared to those obtained from the experimental samples. Key values such as peak temperature (see Table 3) are identified and compared. Heating and cooling rates are calculated at 5-minute intervals for an approximation. The maximum heating and cooling values are identified and compared (see Table 4 and Table 5).

The LS-DYNA 2D models are able to predict peak temperatures with minimum 90% of their experimentally recorded values. Heating and cooling rates are able to be predicted with minimum 60% of their experimentally recorded values.

Table 3. Peak temperature comparison for 2D LS-DYNA analysis

Model	Time to Peak Core Temperature	Experimental Model Peak Temperature [℃]	LS-DYNA 2D Model Peak Temperature [℃]	% Error
S-SS-22	10	596	636	6.68
S-SS-50	33	582	604	3.86
S-GS-74	39	450	453	0.69
L-GS-70	37	488	518	6.17
L-GS-100A	37	408	423	3.72
L-GS-100B	37	418	450	7.54

Table 4. Maximum heating rates comparison for 2D LS-DYNA analysis

Model	Experimental Model Heating Rate $[℃ / sec]$	LS-DYNA 2D Model Heating Rate $[℃ / sec]$	% Error
S-SS-22	1.29	1.51	15.06
S-SS-50	0.55	0.61	10.47
S-GS-74	0.31	0.32	1.23
L-GS-70	0.34	0.39	12.86
L-GS-100A	0.23	0.36	35.74
L-GS-100B	0.23	0.33	31.52

Table 5. Maximum cooling rates comparison for 2D LS-DYNA analysis

Model	Experimental Model Heating Rate $[℃ / sec]$	LS-DYNA 2D Model Cooling Rate $[℃ / sec]$	% Error
S-SS-22	-0.33	-0.33	0.34
S-SS-50	-0.26	-0.29	11.92
S-GS-74	-0.15	-0.11	37.30
L-GS-70	-0.17	-0.20	16.04
L-GS-100A	-0.13	-0.11	19.35
L-GS-100B	-0.12	-0.14	13.46

4. Conclusions and Future Research

This paper presents a novel methodology for capturing the thermal response of spiral and locked-coil strands subjected to realistic fires. The methodology is validated against a range previous unloaded experiments of large diameter cables and implemented in LS-DYNA. Both 2D and 3D models are analyzed and compared. The results showed that the thermal response of these structural cables can be estimated using 2D models for the scenario considered. Radiation and conduction through the air gaps are shown to be the primary mechanisms for heat transfer between the strands. The proposed methodology is tested on the spiral strand and locked-coil cables, made out of stainless steel and galvanized steel, ranging from 22 mm to 100 mm in diameter. The model results are plotted against experimental results, demonstrating the model's ability to give conservative estimates for peak temperature values with at least 90% accuracy even with a 2D representation. The core strand temperatures are shown to be highly dependent on the geometry of the cables, notably the distance separating the strands, and the value chosen for thermal conductivity. Analyses performed with a densely packed geometry and thermal conductivity of the air taken at the average temperature experienced are shown to give optimal results.

A model for predicting the heat transfer in cables can be used to estimate material degradation during and after a fire event, as simplified analysis cannot accurately predict the material degradation, and therefore, the expected level of damage of structural cables exposed to fire [9]. Practitioners can use the methodology described herein to understand the thermal response of unloaded structural cables. Developing an understanding of the temperature distribution in a cable cross-section allows subsequent estimation of the resulting strains and deformations in the structure and ensures its resilience in a fire event.

Additional analysis is required to validate the model against other standard structural cable cross-sections, such as wire rope strands and parallel strand cables [6]. Verifying the model against other geometries ensures it can be used to estimate the thermal response of any commercially available structural cable. Analyzing different geometries can also confirm the main mechanics for heat transfer, or identify any new ones to refine further the methodology presented herein. Completing this research may require the additional experimental task of testing a larger sample size of cables, thus allowing for the statistical analysis of heat transfer results.

The methodology presented herein serves as a building block for developing a more robust framework to predict the thermomechanical response of structural cables under a variety of fire conditions. The larger framework undertaken by the authors will culminate in a coupled thermostructural analysis tool for cable elements, a need identified by multiple authors [6]. This experimental and numerical framework follows the progression of experimentally testing and numerically modelling the thermal response of structural cables to localized heating, conducting structural tests and numerical validation of cable members under induced thermal straining, and finally conducting and modelling the results of combined mechanical and thermal experiments to complete the coupled thermostructural model. This novel framework will result in more advanced tools for practitioners to conduct performance-based fire design of cable-supported structures and provides much-needed knowledge of the thermomechanical response of cable elements which currently has limited available guidance. Ultimately this research contributes to the development of fire-resilient critical infrastructure.

The novelty of this study is twofold. First, this modelling study is the first to consider the thermal response of locked-coil and spiral-strand cables under localized heating from a pool fire, a credible fire exposure case for cable-supported bridges. Second, this work contributes to further understanding and representing the novel observations of the experimental study by Nicoletta et al. which are also in-line with the critical second-order effects of cable uncoiling and thermally-induced moments identified by Kotsovinos et al. [6, 15]. This work contributes to the initial step of characterizing the heat transfer of cable elements under non-uniform heating required to further understand the complex thermomechanical actions of cables exposed to fire.

Acknowledgements

Organizations thanked for their contributions include the Arup UK Fire Group, the NSERC ALLIANCE program (A2021-0148) and Lassonde Undergraduate Student Awards programme. Bronwyn Chorlton and Robert Reynolds are also thanked for their assistance in troubleshooting with software. Aurora Wang and Emma Bresil are thanked for their copy editing of the manuscript.

References

[1] Y. Du, J. Y. Richard Liew, H. Zhang, and Guoqiang-Li, “Pre-tensioned steel cables exposed to fires,” *Advanced Steel Construction*, vol. 14, no. 2, pp. 206–226, 2018, doi: 10.18057/IJASC.2018.14.2.5.

[2] M. Z. Naser and V. K. R. Kodur, “A probabilistic assessment for classification of bridges against fire hazard,” *Fire Safety Journal*, vol. 76, pp. 65–73, Jun. 2015, doi: 10.1016/j.firesaf.2015.06.001.

[3] M. Garlock, I. Paya-Zaforteza, V. Kodur, and L. Gu, “Fire hazard in bridges: Review, assessment and repair strategies,” *Engineering Structures*, vol. 35, pp. 89–98, Feb. 2012, doi: 10.1016/j.engstruct.2011.11.002.

[4] S. E. Quiel, T. Yokoyama, L. S. Bregman, K. A. Mueller, and S. M. Marjanishvili, “A streamlined framework for calculating the response of steel-supported bridges to open-air tanker truck fires,” *Fire Safety Journal*, vol. 73, pp. 63–75, Apr. 2015, doi: 10.1016/j.firesaf.2015.03.004.

[5] E. Kragh, H. Narasimhan and J. Laigaard Jensen (2020) Fire Protection of Bridge Cables, Structural Engineering International, 30:4, 530-533, doi: 10.1080/10168664.2020.1716653

[6] P. Kotsovinos, R. Judge, G. Walker, and P. Woodburn, “Fire Performance of Structural Cables: Current Understanding, Knowledge Gaps, and Proposed Research Agenda,” *Journal of Structural Engineering*, vol. 146, no. 8, p. 03120002, Aug. 2020, doi: 10.1061/(asce)st.1943-541x.0002703.

[7] B. Nicoletta, P. Kotsovinos, and J. Gales, “Review of the fire risk, hazard, and thermomechanical response of bridges in fire,” *Canadian Journal of Civil Engineering*, vol. 47, no. 4, pp. 363–381, 2020, doi: 10.1139/cjce-2018-0767.

[8] Bennetts I, Moinuddin K. Evaluation of the impact of potential fire scenarios on structural

elements of a cable-stayed bridge. J Fire Prot Eng. 2009; 19(2), 85–106. doi:10.1177/

1042391508095091.

[9] Liu YJ., Ning B, Wang Y. Study on thermal and structural behaviour of a cable-stayed bridge under potential Tanker truck fires. App Mech Mater. 2012; 238(2012): 684–688.

[10] Gong X, Agrawal A. K. Safety of cable-supported bridges during fire hazards. J Bridge Eng.
2016; 21(4), 04015082. doi:10.1061/(ASCE)BE. 1943-5592.0000870.

[11] Kotsovinos P, Walker G, Flint G, et al.Assessing the Fires on the Deck of Cable Stayed Bridges. Proceedings of the 9th International Conference on Structures in Fire; 2016 Jun 8-19; Princeton, United States, 9.

[12] M. J. Mahesh Politecnico di Torino *et al.*, "Effect Of Dynamic Unloading of Cables in Collapse Progression Through a Cable Stayed Bridge," 2016. Online]. Available: https://www.researchgate.net/publication/295869529

[13] C. Jeanneret, B. Nicoletta, L. Robertson, J. Gales, and P. Kotsovinos, "Guidance for the post-fire structural assessment of prestressing steel," *Engineering Structures*, vol. 235, May 2021, doi: 10.1016/j.engstruct.2021.112023.

[14] Milne C, "Fire Performance of Spiral Strand Steel Cables," 2016. doi: 10.13140/RG.2.2.34712.11520.

[15] B. Nicoletta, J. Gales, P. Kotsovinos, and B. Weckman, "Experimental Thermal Performance of Unloaded Spiral Strand and Locked-Coil Cables Subject to Pool Fires," *Structural Engineering International*, 2021, doi: 10.1080/10168664.2021.1881943.

[16] E. Mitsoulis and J. Vlachopoulos, "The finite element method for flow and heat transfer analysis," *Advances in Polymer Technology*, vol. 4, no. 2, pp. 107–121, 1984, doi: 10.1002/adv.1984.060040203.

[17] M. A. Rao, M. R. Khanna, K. J. Somaiya, and M. Gangopadhyay, "Applications of Finite Elements Method (FEM) - An Overview," 2012. doi: 10.13140/RG.2.2.36294.42565.

[18] Egle Rackauskaite; Graeme Flint; Ahmed Maani; Alastair Temple; Panagiotis Kotsovinos. (2019). Use of LS-DYNA for Structural Fire Engineering. 12th European LS-DYNA Conference 2019.

[19] B. Nicoletta, "Thermal Performance of Unloaded Spiral Strand and Locked-Coil Cables for Bridge Infrastructure," Toronto, Aug. 2020.

[20] P. Kotsovinos, A. Atalioti, N. McSwiney, F. Lugaresi, G. Rein, and A. J. Sadowski, "Analysis of the Thermomechanical Response of Structural Cables Subject to Fire," *Fire Technology*, vol. 56, no. 2, pp. 515–543, Mar. 2020, doi: 10.1007/s10694-019-00889-7.

[21] F. Lugaresi, "Validation of Models for Structural Steel Cables in Fire," 2017.

[22] V. Fontanari, M. Benedetti, B. D. Monelli, and F. Degasperi, "Fire behavior of steel wire ropes: Experimental investigation and numerical analysis," *Engineering Structures*, vol. 84, pp. 340–349, Feb. 2015, doi: 10.1016/j.engstruct.2014.12.004.

[23] S. Quiel, T. Yokoyama, K. Mueller, L. Bregman, and S. Marjanishvili, "Mitigating the Effects of a Tanker Truck Fire on a Cable-Stayed Bridge," in *International Conference on Performance-based and Life-cycle Structural Engineering*, 2015, pp. 1002–1012. doi: 10.14264/UQL.2016.539.

[24] V. Fontanari, M. Benedetti, and B. D. Monelli, “Elasto-plastic behavior of a Warrington-Seale rope: Experimental analysis and finite element modeling,” *Engineering Structures*, vol. 82, pp. 113–120, Jan. 2015, doi: 10.1016/j.engstruct.2014.10.032.

[25] Bridon structural systems catalogue, 11/2007, Edition 3.

[26] Altair University, “Introduction to Meshing,” 2014. Accessed: Aug. 09, 2021. Online]. Available: https://altairuniversity.com/wp-content/uploads/2014/02/meshing.pdf

[27] Eurpoean Committee for Standardization, “EN 1993-1-2: Eurocode 3: Design of steel structures - Part 1-2: General rules - Structural fire design,” 1993.

[28] D. R. Askeland, P. P. Fulay, and W. J. Wright, *The Science and Engineering of Materials*, 6th ed. Stamford: Global Engineering, 2010.

[29] Kvs. Rao, K. G. Girisha, P. R. Shree, and M. Kumar, “Effect of Surface Coatings on Thermal performance of steel Substrates,” 2017. Online]. Available: www.sciencedirect.comwww.materialstoday.com/proceedings2214-7853

[30] LSTC, “Volume I Keyword,” 1992. Online]. Available: www.lstc.com

[31] E. Rackauskaite, P. Kotsovinos, and G. Rein, “Model parameter sensitivity and benchmarking of the explicit dynamic solver of LS-DYNA for structural analysis in case of fire,” *Fire Safety Journal*, vol. 90, pp. 123–138, Jun. 2017, doi: 10.1016/j.firesaf.2017.03.002.

[32] A. Shapiro, “Using LS-DYNA for Heat Transfer & Coupled Thermal-Stress Problems,” 2012. Accessed: Aug. 09, 2021. Online]. Available: https://ftp.lstc.com/anonymous/outgoing/support/FAQ_docs/heat_transfer_class.pdf